Supporting information

The impact of aerosol size-dependent hygroscopicity and mixing state on the cloud condensation nuclei potential over the Northeast Atlantic

Wei Xu[1,2], Kirsten N. Fossum[1], Jurgita Ovadnevaite[1], Chunshui Lin[1,2], Ru-Jin Huang[2], Colin O'Dowd[1], Darius Ceburnis[1]

[1]School of Physics, Ryan Institute's Centre for Climate and Air Pollution Studies, National University of Ireland Galway, Galway, Ireland.

[2]State Key Laboratory of Loess and Quaternary Geology and Key Laboratory of Aerosol Chemistry and Physics, Institute of Earth Environment, Chinese Academy of Sciences, Xi'an, China.

Correspondence to: Ru-Jin. Huang (rujin.huang@ieecas.cn) and Colin O'Dowd (colin.odowd@nuigalway.ie)

Content

Table S1. The arithmetic mean (standard deviation) of predicted N_{CCN} by each method in different types of air masses.

sector	supersaturation	A	B	C	D	E	F
Clean-H	0.25% SS	97(43)	115(53)	110(48)	107(47)	107(47)	106(47)
	0.5% SS	146(88)	212(125)	212(118)	170(97)	176(101)	173(98)
	0.75% SS	211(127)	326(177)	346(177)	287(155)	287(154)	279(150)
	1% SS	424(199)	539(272)	556(282)	505(254)	502(253)	495(248)
Clean-L	0.25% SS	143(79)	171(100)	162(90)	156(87)	155(87)	153(85)
	0.5% SS	202(130)	294(186)	279(172)	224(149)	228(151)	223(146)
	0.75% SS	289(186)	422(238)	430(238)	337(211)	340(211)	333(207)
	1% SS	373(219)	474(271)	486(277)	412(247)	406(248)	399(243)
Mix-H	0.25% SS	233(157)	267(175)	249(162)	231(149)	227(146)	224(141)
	0.5% SS	371(293)	448(329)	435(327)	365(271)	359(260)	354(253)
	0.75% SS	491(388)	593(418)	597(426)	504(370)	497(360)	488(352)
	1% SS	620(491)	706(522)	728(551)	625(461)	616(457)	603(446)
Mix-L	0.25% SS	679(767)	752(858)	636(737)	595(716)	570(698)	559(691)
	0.5% SS	1041(1221)	1129(1267)	1023(1196)	925(1141)	897(1133)	870(1112)
	0.75% SS	1267(1426)	1385(1480)	1298(1423)	1174(1361)	1152(1361)	1114(1341)
	1% SS	1405(1638)	1504(1655)	1419(1568)	1279(1507)	1255(1498)	1214(1478)
Polluted-H	0.25% SS	564(418)	601(416)	538(376)	485(351)	467(334)	455(322)
	0.5% SS	1019(691)	1096(673)	1036(642)	869(587)	833(558)	804(522)
	0.75% SS	1335(827)	1424(817)	1411(808)	1210(728)	1152(708)	1114(656)
	1% SS	1604(858)	1668(843)	1689(842)	1477(752)	1436(744)	1351(687)
Polluted-L	0.25% SS	1465(1039)	1442(1034)	1154(922)	1061(889)	975(863)	952(848)
	0.5% SS	2343(1530)	2309(1463)	2040(1355)	1793(1308)	1692(1287)	1608(1251)
	0.75% SS	2830(1768)	2825(1685)	2622(1601)	2328(1555)	2244(1539)	2108(1482)
	1% SS	3379(2188)	3322(1929)	3141(1861)	2834(1790)	2768(1785)	2583(1722)

Table S2. The mass concentration (ng m^{-3}) of chemical composition and κ_{chem} in each type of air mass (arithmetic mean ± standard deviation).

sector	κ_{chem}	BC	Org	$nss-SO_4$	sea-salt	MSA	NH_4	NO_3
Clean-H	0.64±0.087	7±3.8	120±160	340±210	170±130	36±31	28±15	9.7±3.1
Clean-L	0.84±0.094	6.5±4.2	55±41	110±61	430±270	1.3±0.79	10±7.3	16±6.3
Mixed-H	0.56±0.11	49±410	250±260	660±690	120±110	54±49	100±100	26±27
Mixed-L	0.57±0.21	84±130	510±860	270±380	280±220	2.9±3	96±230	140±390
Polluted-H	0.4±0.087	100±83	880±840	760±560	35±63	48±31	260±230	200±270
Polluted-L	0.33±0.097	320±200	2700±1700	990±620	76±87	5.5±3.8	510±400	760±810

Table S3. The κ_{HTDMA} in each type of air mass (arithmetic mean ± standard deviation).

sector	035nm	050nm	075nm	110nm	165nm
Clean-H	0.523±0.06	0.476±0.09	0.496±0.1	0.478±0.09	0.495±0.08
Clean-L	0.342±0.1	0.396±0.2	0.515±0.1	0.556±0.1	0.601±0.1
Mixed-H	0.364±0.1	0.335±0.1	0.332±0.1	0.354±0.09	0.389±0.09
Mixed-L	0.247±0.2	0.25±0.2	0.273±0.2	0.289±0.2	0.322±0.2
Polluted-H	0.26±0.09	0.25±0.08	0.226±0.07	0.253±0.08	0.287±0.08
Polluted-L	0.146±0.05	0.139±0.05	0.13±0.06	0.154±0.08	0.183±0.09

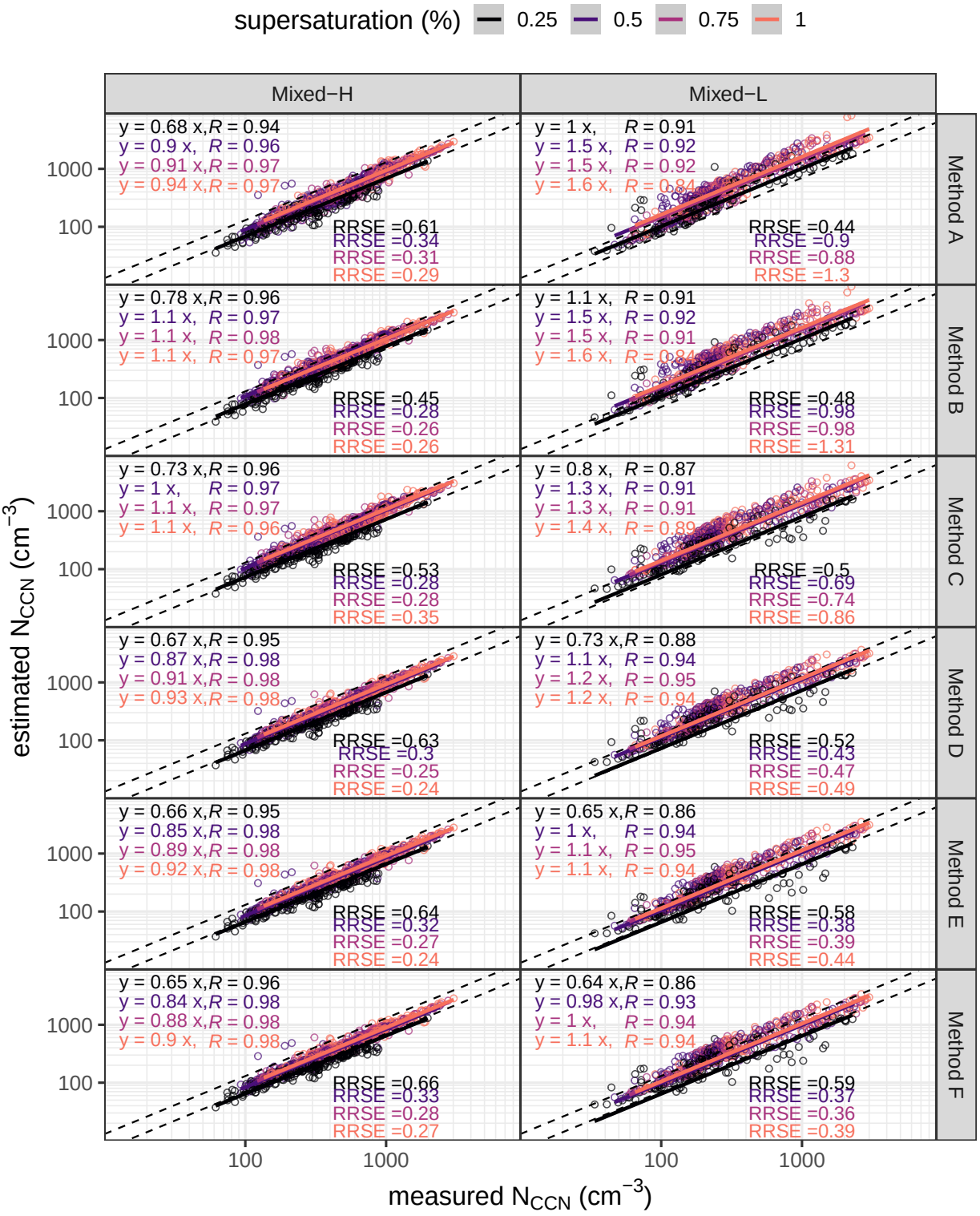

Figure S1. Comparison of measured NCCN against estimated NCCN under different SS using each method in Mixed-L and Mixed-H. The colour codes represent SS, equation of regression line, Pearson correlation efficient and relative root square error (RRSE) are shown in each panel. The dashed lines represent 30% uncertainty ranges. To note that axes are in logarithmic

scales.

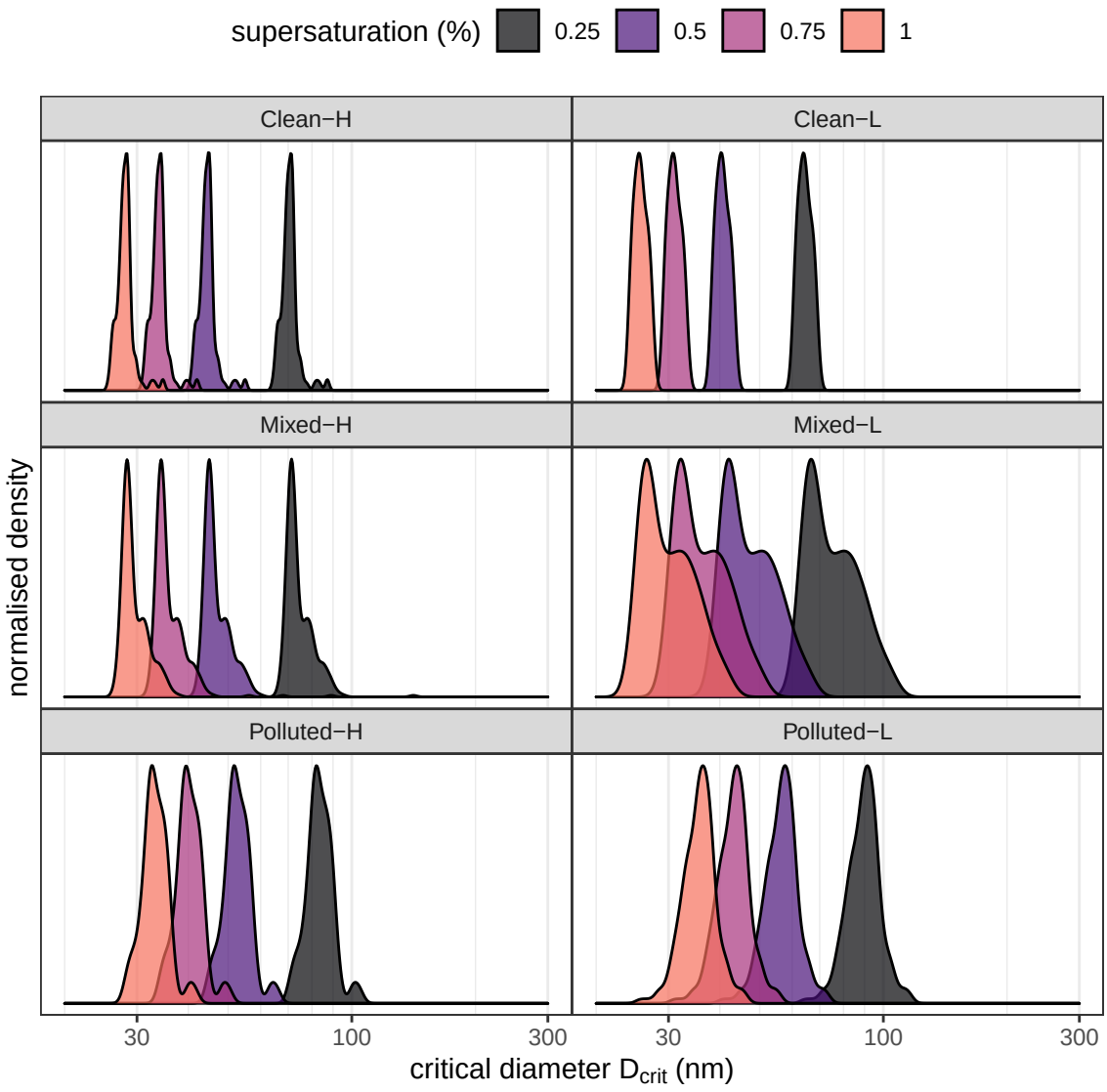

Figure S2. The normalised frequency of distribution of critical diameter (D_{crit}, nm) obtained by method A (chemical composition) for different types of air masses.

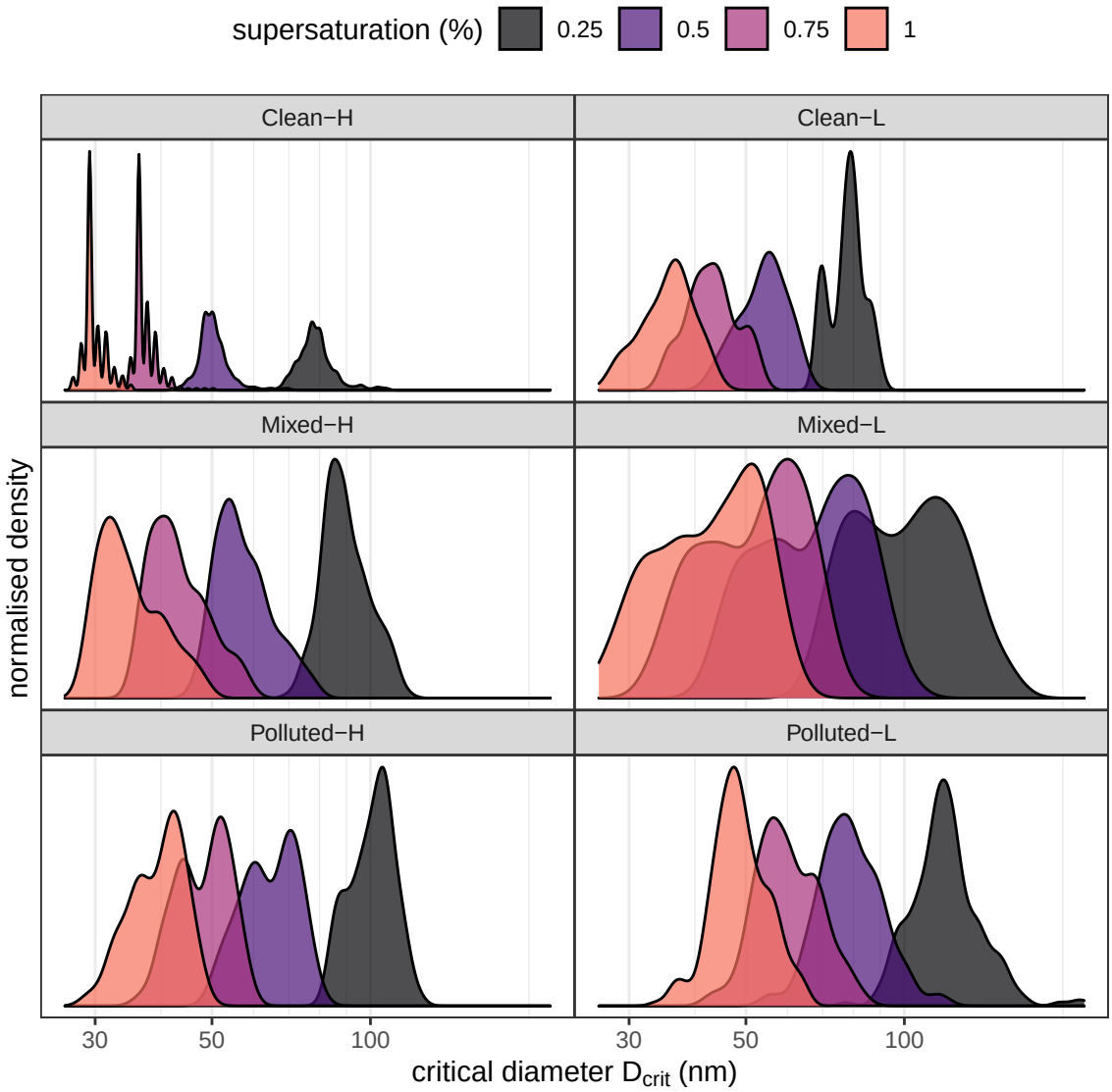

Figure S3. The normalised frequency of distribution of critical diameter (D_{crit}, nm) obtained by method D (size dependent growth factor) for different types of air masses.

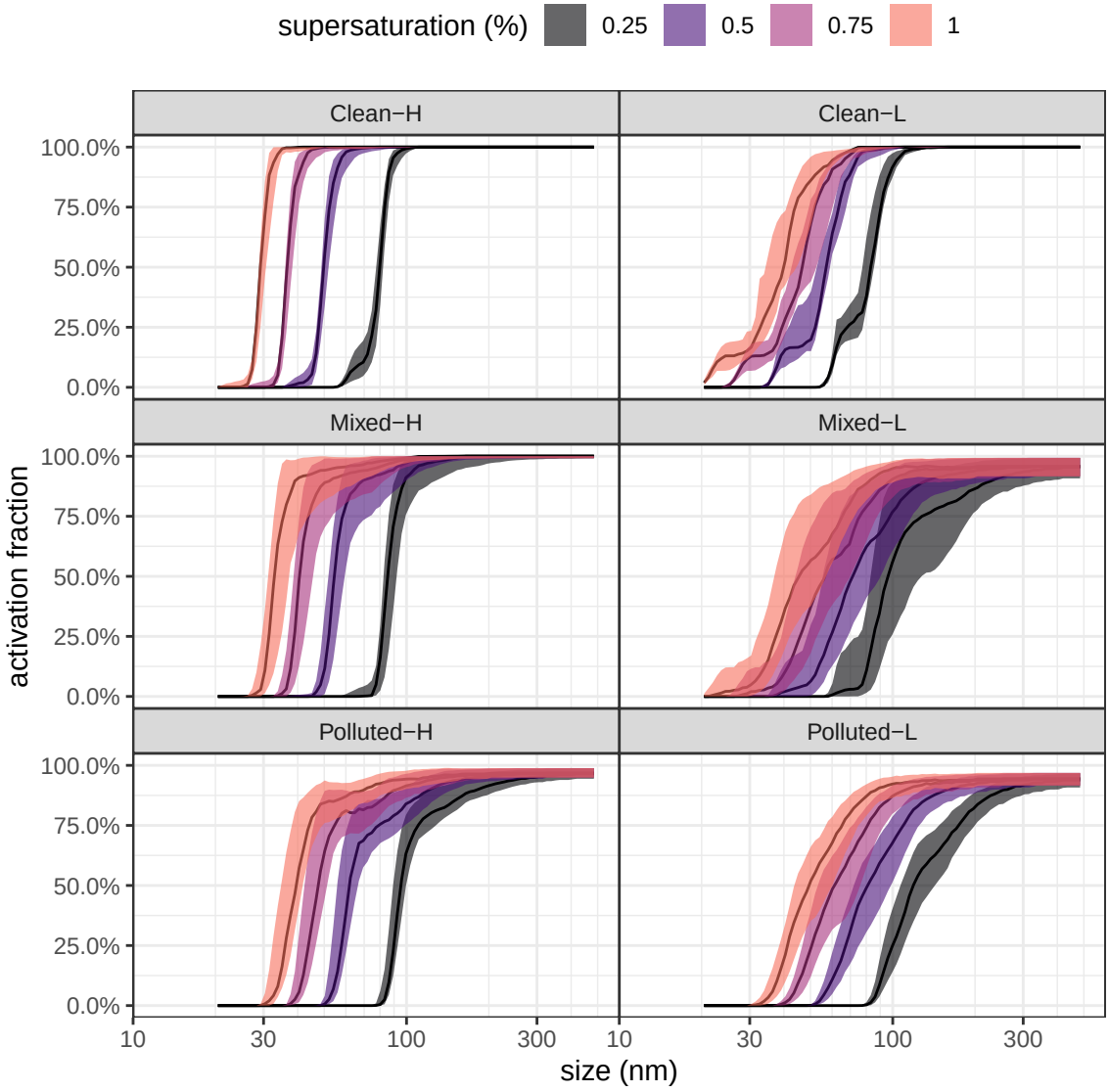

Figure S4. Size resolved activation fraction obtained by method F (growth factor- probability density function, GF-PDF) for different types of air masses. The lines represent median activation fractions, the shaded area represents 25th to 75th percentiles. The colours represent different supersaturations.

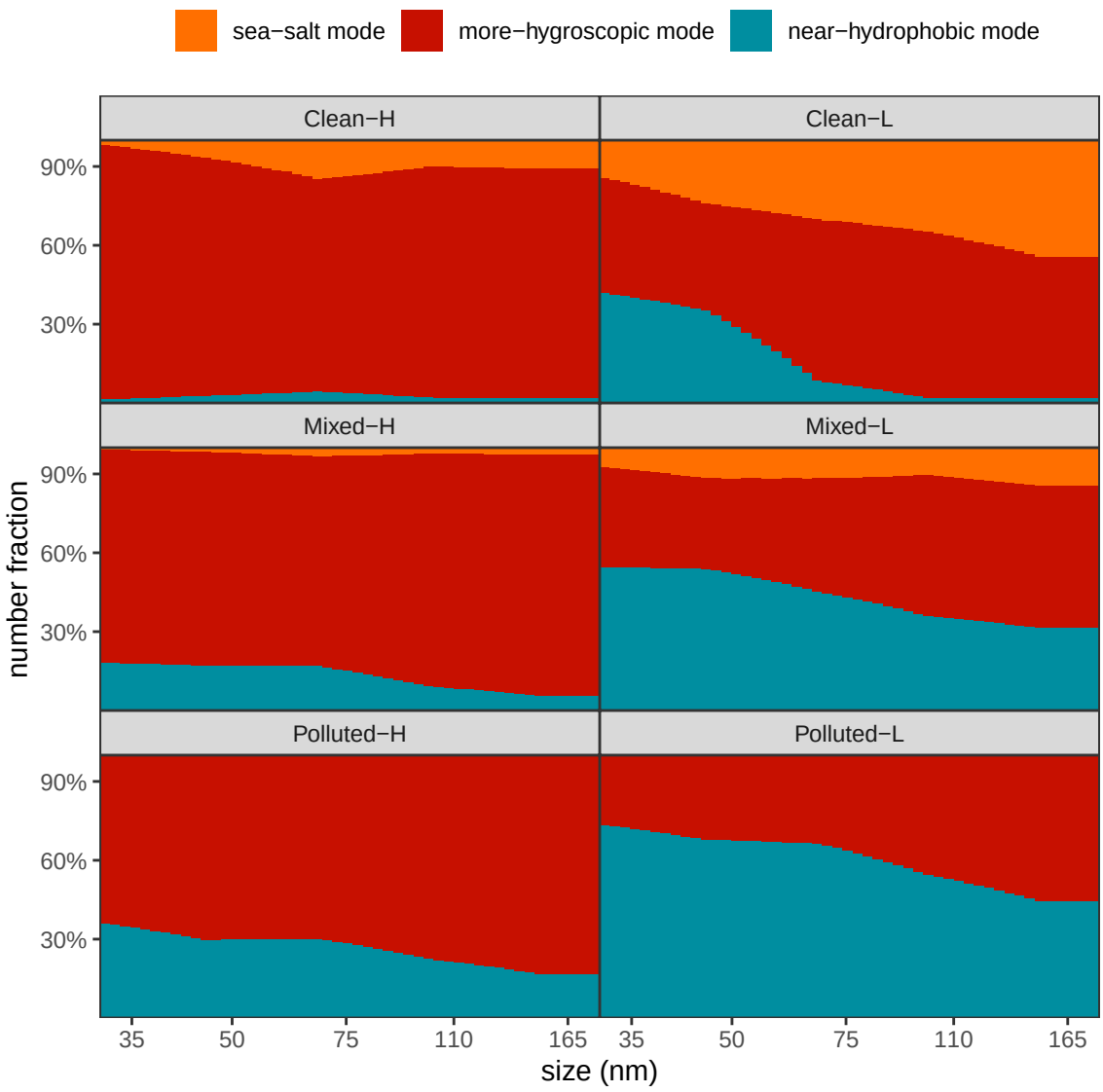

Figure S5. The size resolved number fractions of near-hydrophobic (NH, blue), more-hygroscopic (MH, red) and sea-salt (SS, orange) modes for different types of air masses used in method D.

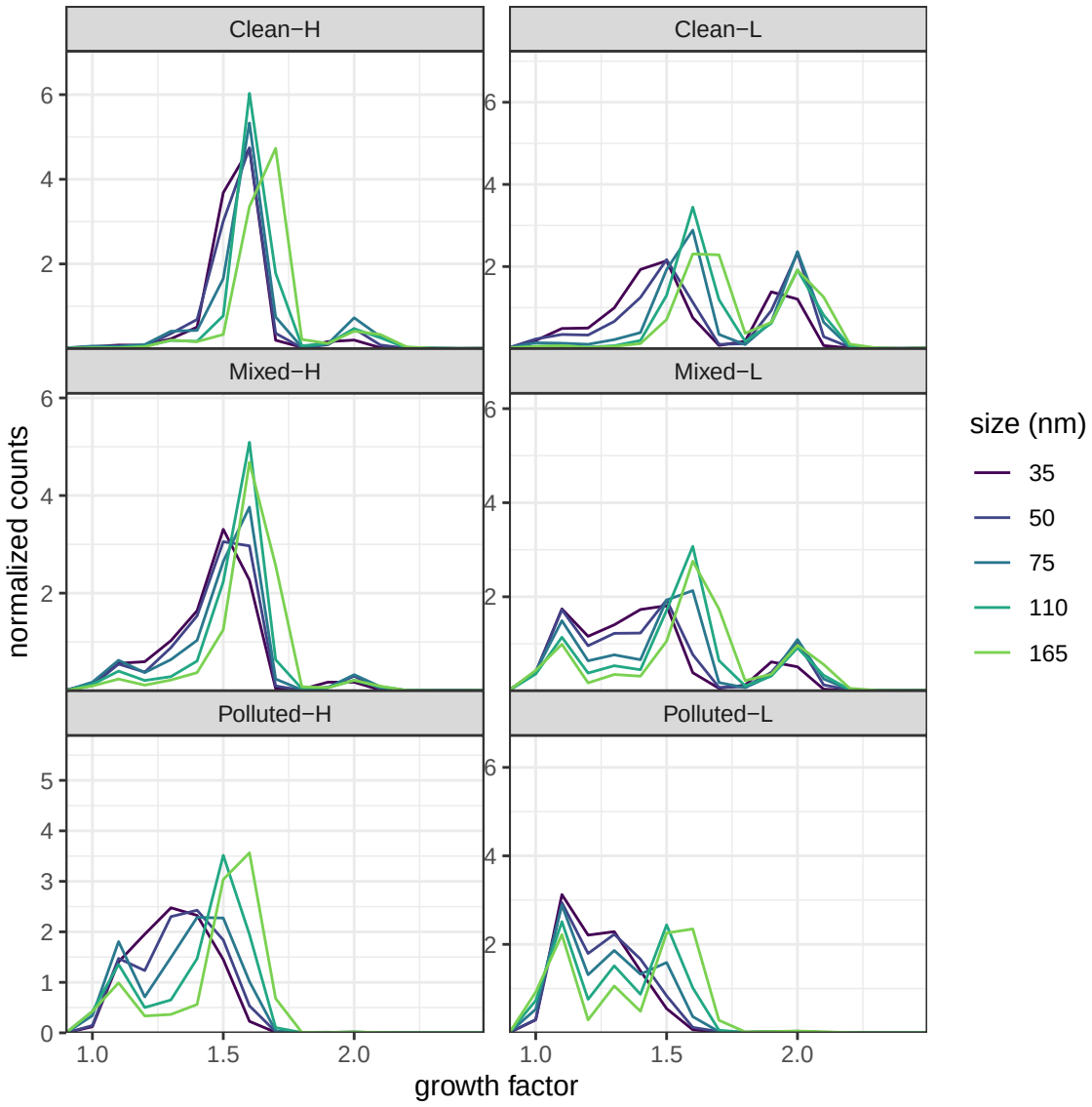

Figure S6. The averaged growth-factor probability density function for different types of air masses.